Recent results on charmed baryons from Belle

Suxian Li (on behalf of the Belle Collaboration)[1,*]

[1]Institute of Modern Physics, Fudan University, Shanghai, China

Abstract. Charmed baryon spectroscopy can provide unique insights into QCD at low energies. The large data sample accumulated by the Belle experiment at the KEKB asymmetric-energy e^+e^- collider enables new opportunities to study charmed baryons. We present recent measurements of charmed baryons at Belle, including studies of $\Lambda_c^+ \to \Sigma^+\eta(')$, $\Lambda_c^+ \to pK_S^0K_S^0/pK_S^0\eta$, $\Omega_c^0 \to \Xi^-\pi^+/\Xi^-K^+/\Omega^-K^+$, and recent results on the properties of the excited state $\Lambda_c(2625)^+$.

1 Introduction

The hadronic weak decays of charmed baryons provide an excellent platform for understanding the quantum chromodynamics with transitions involving the charm quark. The decay amplitude can be decomposed into factorizable and non-factorizable contributions. The latter may play an essential role and are approached in various ways, including the pole model [1], the covariant confined quark model [2], current algebra [3] and $SU(3)_F$ symmetry [4]. To date, there is no good phenomenological model to consistently describe the baryon decays. Precise measurements of the charmed baryon weak decays are helpful to study the dynamics of charmed baryons and to test the predictions of theoretical models.

The Belle experiment ran at the KEKB e^+e^- collider [5]. The Belle detector [6] is a large-solid-angle magnetic spectrometer that consists of a silicon vertex detector, a central drift chamber, an aerogel threshold Cherenkov counter, a time-of-flight scintillation counter, and an electromagnetic calorimeter located inside a superconducting solenoid coil that provides a 1.5 T magnetic field. An iron flux-return located outside of the coil is instrumented to detect K_L^0 mesons and to identify muons.

Charmed baryons can be produced by charm production process $e^+e^- \to c\bar{c}$, and also by the decay of bottom mesons and baryons like B, B_s, Λ_b. Belle accumulated her final data set of integrated luminosity around 1 ab^{-1}, which provides a large charm sample to study charm physics. In this proceeding, we present four selected recent results from Belle on charmed baryons.

2 Branching fractions and asymmetry parameters of $\Lambda_c^+ \to \Sigma^+ h^0$ ($h^0 = \pi^0,\ \eta,\ \eta'$)

This measurement has been performed using the full Belle data sets. Three decay modes $\Lambda_c^+ \to \Sigma^+\pi^0$, $\Sigma^+\eta$, and $\Sigma^+\eta'$ are studied, where Σ^+ is reconstructed with $\Sigma^+ \to p\pi^0$, η' is

*e-mail: lisuxian@fudan.edu.cn

reconstructed with $\eta' \to \eta\pi^+\pi^-$, and η/π^0 is reconstructed with $\eta/\pi^0 \to \gamma\gamma$ [7]. For branching fraction measurements, the $\Lambda_c^+ \to \Sigma^+\pi^0$ is used as a normalization mode, and the branching ratios relative to this mode are measured. The Λ_c^+ signal yields are extracted by performing fits to the $M(\Sigma^+h^0)$ mass spectra, which are shown in figure 1. Taking $\mathcal{B}(\Lambda_c^+ \to \Sigma^+\pi^0) = (1.25 \pm 0.10)\%$ [8], the absolute branching fractions are measured to be

$$\mathcal{B}(\Lambda_c^+ \to \Sigma^+\eta) = (3.14 \pm 0.35 \pm 0.11 \pm 0.25) \times 10^{-3},$$
$$\mathcal{B}(\Lambda_c^+ \to \Sigma^+\eta') = (4.16 \pm 0.75 \pm 0.21 \pm 0.33) \times 10^{-3},$$

where the third uncertainty is from $\mathcal{B}(\Lambda_c^+ \to \Sigma^+\pi^0)$. The measured results are the most precise results to date and agree with previous results [8] within two standard deviations. Comparing with the theoretical predictions based on pole model, quark model, current algebra, and $SU(3)_F$ symmetry [1–4], none of theoretical methods could predict the $\mathcal{B}(\Lambda_c^+ \to \Sigma^+\eta')$ well and only results using quark model is basically consistent with the measured $\mathcal{B}(\Lambda_c^+ \to \Sigma^+\eta)$.

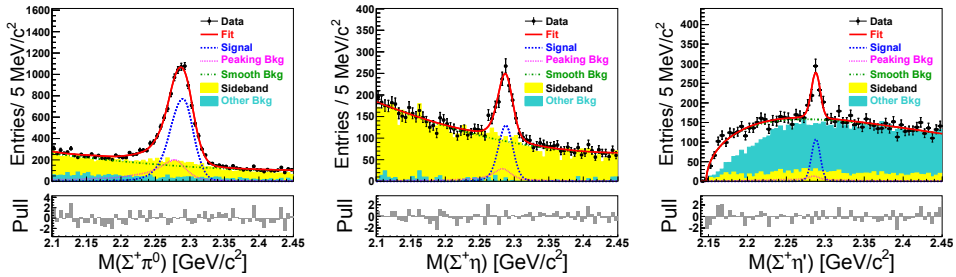

Figure 1. Invariant mass distributions of Σ^+h^0 from data. The black dots with error bars represent the data. The red solid line stands for the overall fit [7].

The weak decay asymmetry parameter $\alpha(\Sigma^+h^0)$ of the $\Lambda_c^+ \to \Sigma^+h^0$ decay determines the differential decay rate as $\frac{dN}{d\cos\theta_{\Sigma^+}} \propto 1 + \alpha(\Sigma^+h^0)\alpha(p\pi^0)\cos\theta_{\Sigma^+}$ [9], where θ_{Σ^+} is the angle between the proton momentum vector and the opposite of the Λ_c^+ momentum vector in the Σ^+ rest frame [10] and $\alpha(p\pi^0) = -0.983 \pm 0.013$ is the averaged asymmetry parameter of $\Sigma^+ \to p\pi^0$ and its charge-conjugated mode [8]. The efficiency-corrected angular distribution for $\Lambda_c^+ \to \Sigma^+h^0$ are shown in figure 2 and the asymmetry parameters are obtained by fitting these distributions. The measured asymmetry parameters are

$$\alpha(\Sigma^+\pi^0) = -0.48 \pm 0.02 \pm 0.02,$$
$$\alpha(\Sigma^+\eta) = -0.99 \pm 0.03 \pm 0.05,$$
$$\alpha(\Sigma^+\eta') = -0.46 \pm 0.06 \pm 0.03,$$

where the first result agrees with the world average value [8] with the uncertainty considerably improved from 20% to 6% and the last two are measured for the first time. Comparing the measured $\alpha(\Sigma^+\pi^0)$ with $\alpha(\Sigma^0\pi^+)$ [8], their agreement within 1σ shows consistency with the prediction from isospin symmetry [4].

3 Branching fractions of $\Lambda_c^+ \to pK_S^0K_S^0$ and $\Lambda_c^+ \to pK_S^0\eta$

The singly Cabibbo-suppressed decay $\Lambda_c^+ \to pK_S^0K_S^0$ and the Cabibbo-favored decay $\Lambda_c^+ \to pK_S^0\eta$ are studied using the full Belle data sets. The K_S^0 is reconstructed with $K_S^0 \to \pi^+\pi^-$ and

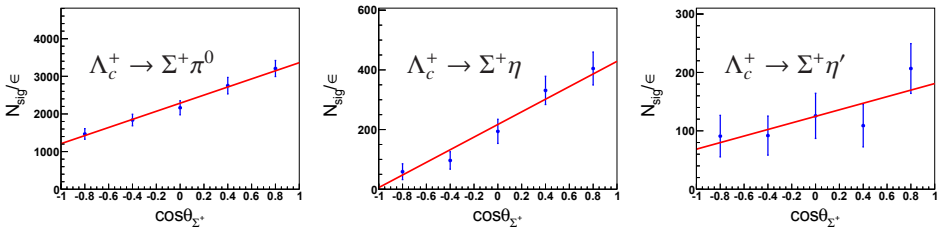

Figure 2. The maximum likelihood fits to the efficiency-corrected $\cos\theta_{\Sigma^+}$ distributions of data to extract the asymmetry parameters [7].

η is reconstructed with $\eta \to \gamma\gamma$. The decay $\Lambda_c^+ \to pK_S^0$ is used as a normalization mode, and the branching ratios relative to this mode are measured [11].

Since the efficiencies of the signal modes are not uniform over the Dalitz plot, the analysis uses a model independent approach to divide the data into 7×7 bins for $\Lambda_c^+ \to pK_S^0K_S^0$ and 5×5 bins for $\Lambda_c^+ \to pK_S^0\eta$ in the Dalitz distribution and to estimate the signal yields and the efficiency in each bin. Signal yields are extracted from the fit to the Λ_c^+ mass distributions. The overall Λ_c^+ mass distributions and the best fit results are shown in figure 3. Using $\mathcal{B}(\Lambda_c^+ \to pK_S^0) = (1.59 \pm 0.08)\%$ [8], the branching fractions of $\Lambda_c^+ \to pK_S^0K_S^0$ and $\Lambda_c^+ \to pK_S^0\eta$ are calculated to be

$$\mathcal{B}(\Lambda_c^+ \to pK_S^0K_S^0) = (2.35 \pm 0.12 \pm 0.07 \pm 0.12) \times 10^{-4},$$
$$\mathcal{B}(\Lambda_c^+ \to pK_S^0\eta) = (4.35 \pm 0.10 \pm 0.20 \pm 0.22) \times 10^{-3},$$

where the third errors are from the uncertainty of $\mathcal{B}(\Lambda_c^+ \to pK_S^0)$. The branching fraction of $\Lambda_c^+ \to pK_S^0K_S^0$ is measured for the first time and the result for the other mode is more precise than previous measurements.

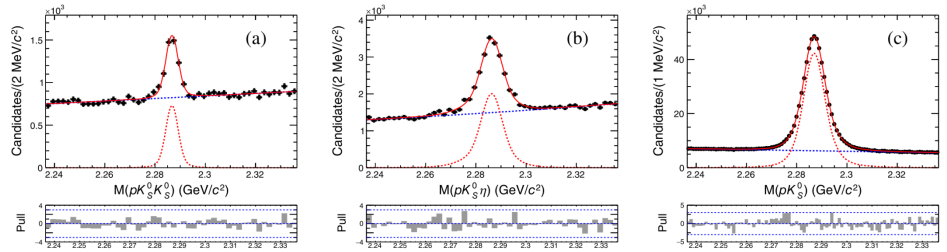

Figure 3. The distributions of invariant mass of Λ_c^+ candidates (points with error bars) and corresponding fit results (red curves) for (a) $\Lambda_c^+ \to pK_S^0K_S^0$, (b) $\Lambda_c^+ \to pK_S^0\eta$, and (c) $\Lambda_c^+ \to pK_S^0$ respectively. The red (blue) dashed histograms show the signal (background)[11].

Two clear structures that are consistent with $f_0(980) \to K_S^0K_S^0$ or $a_0(980) \to K_S^0K_S^0$ and $N^*(1535) \to p\eta$ are found in the Dalitz plots for $\Lambda_c^+ \to pK_S^0K_S^0$ and $\Lambda_c^+ \to pK_S^0\eta$, raising the expectation that the nature of these intermediate resonances will be probed in the future with amplitude analyses on the larger datasets anticipated from BESIII and Belle II.

4 Mass and width of $\Lambda_c(2625)^+$ and the branching ratios of $\Lambda_c(2625)^+ \to \Sigma_c^{0,++}\pi^{+,-}$

The $\Lambda_c(2625)^+$ is the excited state of Λ_c^+ and it dominantly decays to $\Lambda_c^+\pi^+\pi^-$ via P-wave decay. The D-wave decay $\Lambda_c(2625)^+ \to \Sigma_c^{0,++}\pi^{+,-}$ is also allowed, but its contribution is known to be small. This analysis is performed by reconstructing the $\Lambda_c(2625)^+ \to \Lambda_c^+\pi^+\pi^-$ using the full Belle data sets, where the Λ_c^+ is reconstructed with $\Lambda_c^+ \to pK^-\pi^+$ [12]. The mass and width of $\Lambda_c(2625)^+$ are obtained by fitting to the $M(\Lambda_c^+\pi^+\pi^-)$ distribution. The mass of the $\Lambda_c(2625)^+$, relative to the Λ_c^+ mass, is determined to be $M(\Lambda_c(2625)^+) - M(\Lambda_c^+) = 341.518 \pm 0.006 \pm 0.049$ MeV/c^2, which is consistent with the past measurement but with approximately half the uncertainty. The upper limit on the width is determined to be $\Gamma(\Lambda_c(2625)^+) < 0.52$ MeV/c^2 at 90% confidence level, which is around a factor of 2 more stringent than the previous limit.

A Dalitz plot fit is made in order to determine the branching ratios of $\Lambda_c(2625)^+$ with respect to the mode $\Lambda_c(2625)^+ \to \Lambda_c^+\pi^+\pi^-$, using an amplitude model [13]. The $\Lambda_c(2625)^+$ signal distribution is calculated from the squared amplitude with spin sum of final states and spin average of the initial states via $\sum|T_1 + T_2 + T_3 + T_4 + T_5|^2$, where $T_1 - T_5$ are the decay amplitudes through the Σ_c^0, $\Sigma_c(2520)^0$, Σ_c^{++}, $\Sigma_c(2520)^{++}$, and direct three-body decay, respectively. The yield of each decay channel is calculated by an integration of the individual component over the Dalitz plot. Figure 4 shows the projections of the fitted results with each component labeled on the plot. The Σ_c^{++} peak and the reflection peak from Σ_c^0 are evident. The branching ratios relative to the $\Lambda_c(2625)^+ \to \Lambda_c^+\pi^+\pi^-$ are obtained to be

$$\mathcal{B}(\Lambda_c(2625)^+ \to \Sigma_c^0\pi^+)/\mathcal{B}(\Lambda_c(2625)^+ \to \Lambda_c^+\pi^+\pi^-) = (5.19 \pm 0.23 \pm 0.40)\%,$$
$$\mathcal{B}(\Lambda_c(2625)^+ \to \Sigma_c^{++}\pi^-)/\mathcal{B}(\Lambda_c(2625)^+ \to \Lambda_c^+\pi^+\pi^-) = (5.13 \pm 0.26 \pm 0.32)\%.$$

These are the first measurements, as previously only limits have been presented. The results can be used as inputs to theoretical models to generate predictions for other heavy quark baryons.

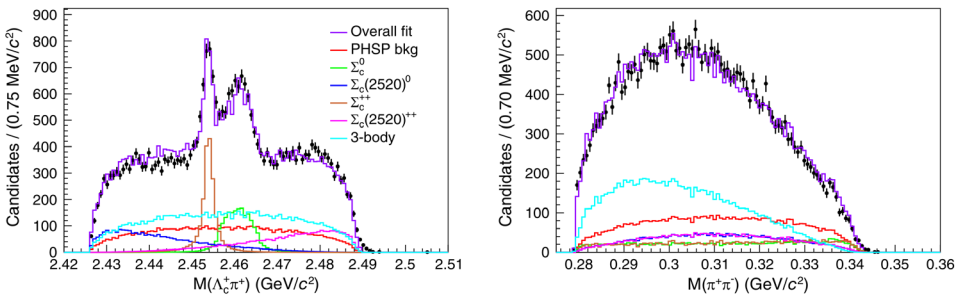

Figure 4. Dalitz plot fit result plotted as projections. Solid lines show the overall fitted distribution and its individual components as indicated in the legend. PHSP refers to phase space [12].

5 Evidence for $\Omega_c^0 \to \Xi^-\pi^+$ and search for $\Omega_c^0 \to \Xi^-K^+$ and $\Omega_c^0 \to \Omega^-K^+$

The singly Cabibbo-suppressed decays $\Omega_c^0 \to \Xi^-\pi^+$ and $\Omega_c^0 \to \Omega^-K^+$ and the doubly Cabibbo-suppressed decay $\Omega_c^0 \to \Xi^-K^+$ are studied using the full Belle data sets, where

the Ξ^- and Ω^- are reconstructed with $\Xi^- \to \Lambda\pi^-$ and $\Omega^- \to \Lambda K^-$, respectively, followed by $\Lambda \to p\pi^-$. The decay $\Omega_c^0 \to \Omega^-\pi^+$ is used as a normalization mode, and the branching ratios relative to this mode are measured [14].

The Ω_c^0 signal yields are extracted by the fit to the Ω_c^0 mass distribution, as shown in figure 5. Evidence for an Ω_c^0 signal in the decay $\Omega_c^0 \to \Xi^-\pi^+$ is reported with a significance of 4.5σ. The ratio of branching fractions to the normalization mode is measured to be

$$\mathcal{B}(\Omega_c^0 \to \Xi^-\pi^+)/\mathcal{B}(\Omega_c^0 \to \Omega^-\pi^+) = (25.3 \pm 5.2 \pm 3.0)\%,$$

which is 2.4σ away from the calculation based on the current algebra and pole methods [15], and larger than the calculation using the light-front quark model [16]. No significant signals of $\Omega_c^0 \to \Xi^-K^+$ and $\Omega_c^0 \to \Omega^-K^+$ are found. The upper limits on branching ratios at 90% confidence level are set to be

$$\mathcal{B}(\Omega_c^0 \to \Xi^-K^+)/\mathcal{B}(\Omega_c^0 \to \Omega^-\pi^+) < 0.07, \quad \mathcal{B}(\Omega_c^0 \to \Omega^-K^+)/\mathcal{B}(\Omega_c^0 \to \Omega^-\pi^+) < 0.29.$$

The former is consistent with the theoretical predictions based on current algebra method and the light-front quark model.

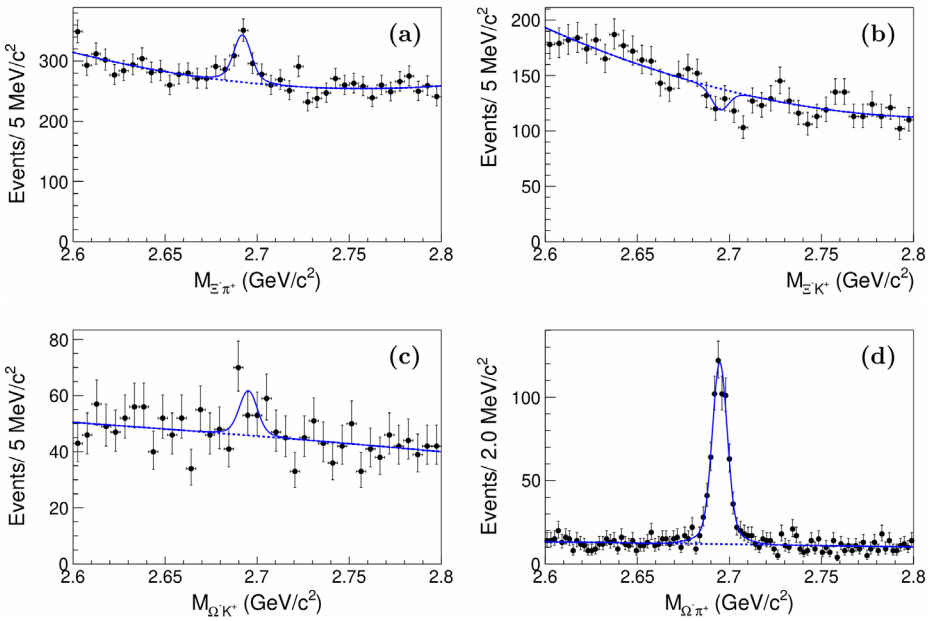

Figure 5. The invariant mass distributions of (a) $\Xi^-\pi^+$, (b) Ξ^-K^+, (c) Ω^-K^+, and (d) $\Omega^-\pi^+$ from data samples. The solid curves are the best fits, and the dashed curves are the fitted backgrounds [14].

6 Summary

Although Belle has stopped data taking for around fifteen years, we are still producing exciting results, especially for charmed baryons. Several selected recent results on charm physics are presented here. These experimental results will be useful to further constrain the parameter space of the theoretical models and can be applied to other heavy quark systems. In the future, Belle II will provide greater sensitivity and precise measurements in charmed baryon physics with 50 ab^{-1}.

References

[1] Q. P. Xu and A. N. Kamal, Phys. Rev. D **46**, 270 (1992); H. Y. Cheng and B. Tseng, Phys. Rev. D **48**, 4188 (1993).

[2] J. G. Korner and M. Kramer, Z. Phys. C **55**, 659 (1992); M. A. Ivanov, J. G. Korner, V. E. Lyubovitskij, and A. G. Rusetsky, Phys. Rev. D **57**, 5632 (1998).

[3] K. K. Sharma and R. C. Verma, Eur. Phys. J. C **7**, 217 (1999); J. Zou, F. Xu, G. Meng, and H. Y. Cheng, Phys. Rev. D **101**, 014011 (2020).

[4] C. D. Lü, W. Wang, and F. S. Yu, Phys. Rev. D **93**, 056008 (2016); C. Q. Geng, C. W. Liu, and T. H. Tsai, Phys. Lett. B **794**, 19 (2019).

[5] S. Kurokawa and E. Kikutani, Nucl. Instrum. Methods Phys. Res., Sect. A **499**, 1 (2003), and other papers included in this Volume; T. Abe *et al.*, Prog. Theor. Exp. Phys. **2013**, 03A001 (2013), and references therein.

[6] A. Abashian *et al.* (Belle Collaboration), Nucl. Instrum. Methods Phys. Res., Sect. A **479**, 117 (2002); also see detector section in J. Brodzicka *et al.*, Prog. Theor. Exp. Phys. **2012**, 04D001 (2012).

[7] S. X. Li, *et al.* (Belle Collaboration), Phys. Rev. D **107**, 032003 (2023).

[8] R. L. Workman *et al.* (Particle Data Group), Prog. Theor. Exp. Phys. **2022**, 083C01 (2022).

[9] R. E. Behrends, Phys. Rev. **111**, 1691 (1958).

[10] P. Bialas, J. G. Körner, M. Krämer, and K. Zalewski, Z. Phys. C **57**, 115 (1993).

[11] L. K. Li, *et al.* (Belle Collaboration), Phys. Rev. D **107**, 032004 (2023).

[12] D. Wang, *et al.* (Belle Collaboration), Phys. Rev. D **107**, 032008 (2023).

[13] A. J. Arifi, H. Nagahiro, and A. Hosaka, Phys. Rev. D **98**, 114007 (2018).

[14] X. Han, *et al.* (Belle Collaboration), J. High Energy Phys. **01**, 055 (2023).

[15] S. Hu, G. Meng and F. Xu, Phys. Rev. D **101**, 094033 (2020).

[16] Z. X. Zhao, Chin. Phys. C **42**, 093101 (2018).